Synthesis, Electrical Conductivity, and Crystal Structure of $Cu_4Sn_7S_{16}$ and Structure Refinement of Cu_2SnS_3

Xue-an Chen, Hiroaki Wada,[1] Akira Sato, and Masahiro Mieno

National Institute for Research in Inorganic Materials, 1-1 Namiki, Tsukuba-shi, Ibaraki 305, Japan

Received November 20, 1997; in revised form March 9, 1998; accepted March 17, 1998

Single crystals of $Cu_4Sn_7S_{16}$ and Cu_2SnS_3 were prepared by the conventional solid state reaction method. Their crystal structures were determined from single-crystal X-ray data. $Cu_4Sn_7S_{16}$ is of a new structure type with rhombohedral symmetry: R-$3m$, $a = 7.372(1)$, $c = 36.010(7)$ Å, $Z = 3$, $R = 0.018$ for 522 structure factors and 36 variable parameters. Its crystal structure may be described as a defect variant of the spinel-type. In the unit cell, 3/4 of the tetrahedral sites and 1/8 of the octahedral sites are occupied by Cu^+, while 7/8 of the octahedral sites are occupied by Sn^{4+} ions. The compound can therefore be formulated as $(Cu_{0.75}\square_{0.25})(Sn_{1.75}Cu_{0.25})S_4$. Cu_2SnS_3 has the unit cell formula $Cu_{2.665(7)}Sn_{1.335(7)}S_4$ ($Z = 2$) and it is isotypic with the tetragonal stannite $[Cu_2(Fe, Zn)SnS_4]$ structure: I-$42m$, $a = 5.413(1)$, $c = 10.824(1)$ Å, $R = 0.030$ for 281 reflections and 16 variables. In the case of Cu_2SnS_3, the positions of the Cu and Sn atoms of stannite are occupied by the composite atoms M1 [43.6(2) at.% Sn + 56.4(2) at.% Cu] and M2 [46.3(3) at.% Sn + 53.7(3) at.% Cu], respectively, while those of the (Fe, Zn) atoms are replaced by only Cu atoms. Electrical conductivity measurements confirm the expected semiconducting behavior of $Cu_4Sn_7S_{16}$, and XPS analysis reveals the presence of only Cu^+ in $Cu_4Sn_7S_{16}$. © 1998 **Academic Press**

INTRODUCTION

The Ag- and Cu-containing chalcogenides are of considerable interest because they exhibit novel structure characteristics and unusual physical properties, e.g., incomplete occupancy of certain Ag or Cu sites causes the order-disorder phenomena and phase transitions (1), and some of these compounds such as Cu_6PS_5Hal (Hal = Cl, Br, I) (1) and $Ag_{3.8}Sn_3S_8$ (2) have high ionic conductivities. The ternary system Cu–Sn–S has been investigated in the past by Khanafer *et al.* (3), Wang (4), Moh (5, 6), and Jaulmes *et al.* (7, 8). Many phases were proposed, and most of them were situated on the Cu_2S–SnS_2 line of this system. For example,

the compounds Cu_4SnS_4, Cu_2SnS_3, "$Cu_2Sn_3S_7$," and $CuSn_{3.75}S_8$ correspond to the Cu_2S mole proportion of 0.6667, 0.50, 0.25, and 0.1176, respectively. Structural characterizations of Cu_4SnS_4 and $CuSn_{3.75}S_8$ have been done by Jaulmes *et al.* (7, 8). Cu_2SnS_3 was found to be dimorphic with a phase transition at 780°C, the high-temperature phase was reported to be isotypic with the cubic ZnS structure, and the low-temperature phase was considered as a triclinic superstructure of sphalerite type (4), while Hahn *et al.* (9) thought that the powder data of the low-temperature phase could be indexed on a tetragonal cell, and Villars *et al.* (10) furthermore assigned the space group I-$42d$ to its structure. The present work confirmed the tetragonal system given by Hahn *et al.*, but with a different space group (I-$42m$). The phase "$Cu_2Sn_3S_7$" was first reported by Wang (4), who predicted that it crystallizes in a monoclinic system with the space group Cc or $C2/c$. In his following work (11), the formula of this compound was redetermined to be $Cu_2Sn_{3.5}S_8$. Our single-crystal structure determination confirmed the revised formula ($Cu_2Sn_{3.5}S_8$) and found the space group actually to be rhombohedral R-$3m$ rather than monoclinic Cc or $C2/c$.

SAMPLE PREPARATION AND CHARACTERIZATION

Starting materials were powders of elements copper, tin, and sulfur, all with nominal purities greater than 99.9%. The compound $Cu_4Sn_7S_{16}$ was synthesized by a stoichiometric mixture of Cu_2S (0.318g, 2.0 mmol, prepared by a stoichiometric reaction of Cu with S at 500°C) and SnS_2 (1.280g, 7.0 mmol, prepared by a stoichiometric reaction of Sn and S at 450°C). The sample was ground in an agate mortar and pressed into pellets. The pellets were introduced into a silica tube and sealed at pressure of less than 10^{-3} Torr. The tubes were held at 450°C for three days, then heated gradually to 850°C, where they were kept for three days, then cooled at a rate of 5°C/h to 600°C and quenched in air. The gray crystals with metallic luster were found in the tubes, and they appear as thin plates of trigonal outlines with a dimension up to 0.5 mm across. As mentioned by

[1] To whom correspondence should be addressed. Fax: 81-298-52-7449. E-mail: wadah@nirim.go.jp.

Wang (4), the parallel growth on the surface plane of the plates is frequently observed. Semiquantitative EDAX analysis with the microprobe of Hitachi S-5000 scanning electron microscope confirmed the presence of all three elements in a ratio of approximately $4.2 : 6.8 : 16$. The compound appears to be relatively stable in air and water. In an alternative tube with a slightly SnS_2-rich composition, both $Cu_4Sn_7S_{16}$ and Sn_2S_3 crystals were observed. The Sn_2S_3 single crystals are easily recognizable as very thin needles.

Cu_2SnS_3 was prepared by a direct reaction of the stoichiometric elements Cu (0.381g, 6.0 mmol), Sn (0.356g, 3.0 mmol), and S (0.289g, 9.0 mmol) at $1050°C$ for two days. The sample was slowly cooled at a rate of $5°C/h$ to $700°C$ and annealed there for two days, then quenched in air. The crystals had the form of prisms with dimensions of up to $0.4 \times 0.4 \times 1.0 \ mm^3$. Microprobe analysis by JEOL JXA-8600 MX gives an approximate atomic ratio $Cu : Sn : S$ of $2 : 1 : 3$, in good agreement with that deduced from the structural refinement.

X-ray powder diffraction intensity data were collected using the graphite-monochromated $CuK\alpha$ radiation of a Rigaku diffractometer (Geigerflex, RAD-2B system). Both compounds were found to be single phases. X-ray diffraction patterns of $Cu_4Sn_7S_{16}$ are in good agreement with those reported by Wang (4) for the monoclinic phase "$Cu_2Sn_3S_7$". It was also possible to index reflection peaks by using a pseudohexagonal cell with dimensions $a_h = 7.371$ Å and $c_h = 36.010$ Å. The symmetry of this compound was finally determined by X-ray single crystal data to be trigonal. X-ray diffraction patterns of Cu_2SnS_3 confirmed the earlier work (9).

X-ray photoelectron spectroscopy (XPS) measurements were performed using a JEOL JPS-9000 MC spectrometer with a $MgK\alpha$ X-ray source ($hv = 1253.6$ eV) in a vacuum of 1×10^{-7} Pa. Powder samples were pressed onto indium foil and then mounted in an aluminum sample holder. The samples were sputtered with an Ar ion beam before the spectra were recorded, and the electron binding energies were referred to the C 1s line of impurity carbon, which had a value of 284.5 eV.

Conductivity measurements of $Cu_4Sn_7S_{16}$ were carried out on rectangular, cold-pressed polycrystalline samples ($2.6 \times 5.0 \times 5.0 \ mm^3$). The experimental cells were built and placed in a special glass container under high purity argon atmosphere. The alternate current method was employed with a Solartron 1286 electrical interface and a Solartron 1255 frequency response analyzer.

STRUCTURE DETERMINATIONS

Single crystals were examined in a Buerger precession camera to establish their symmetry. Overexposed photographs revealed no supercell reflections for both compounds.

The diffraction patterns of $Cu_4Sn_7S_{16}$ showed a rhombohedral cell. The only systematic extinctions (reflections hkl were observed only with $-h + k + l = 3n$) were compatible with the space groups $R3$, $R-3$, $R-32$, $R3m$, and $R-3m$, of which the centrosymmetric group $R-3m$ was found to be correct during the structure refinement. The precession photographs of Cu_2SnS_3 show Laue symmetry $4/mmm$ and the reflection condition hkl : h + k + l = 2n, leading to the possible space groups $I4/mmm$, $I-42m$, $I-4m2$, $I4mm$, and $I422$. With analogy to other chalcopyrite-like compounds, the space group $I-42m$ of acentric symmetry could be adopted as the most probable one.

Intensity data for both compounds were collected on an Enraf-Nonius CAD4 automatic four-circle diffractometer with graphite monochromated $MoK\alpha$ radiation. Cell constants were obtained from a least-squares refinement with 20 automatically centered reflections in the ranges $30° < 2\theta < 50°$ for $Cu_4Sn_7S_{16}$ and $30° < 2\theta < 55°$ for Cu_2SnS_3. Three standard reflections were remeasured after every 200 reflections with no indication of crystal decay. The intensity data were corrected for Lorentz and polarization effects and for absorption by a Gaussian numerical integration using the measured dimensions of the crystal (12). The crystallographic data and some results are summarized in Table 1.

Both structures were solved by direct methods in the SIR-92 program (13) and refined in SHELXL-93 system (14) by full-matrix least-squares methods on F_o^2. The $Cu_4Sn_7S_{16}$ crystal structure was first successfully solved in a monoclinic system based on the lattice constants reported by Wang (4) [$a = 12.772(2)$ Å, $b = 7.371(1)$ Å, $c = 12.736(2)$ Å, and $\beta = 109.53(2)°$]. However, the space group was $C2/m$, $R = 0.022$ for 79 variables and 1226 structure factors. After checking the atomic parameters carefully, we found a missed three-fold axes symmetry. The intensity data was subsequently transformed to a rhombohedral setting by a matrix ($0 -1 0 -1/2 1/2 0 -1 0 -3$) and the structure was finally refined in a trigonal $R-3m$ space group.

For $Cu_4Sn_7S_{16}$, in order to check for deviations from the ideal compositions all occupancy parameters were allowed to vary along with the positional and thermal parameters. The resulting occupancies varied between the values 1.04(3) for Sn2 and 1.07(3) for S2. The only exception was the Cu1 position, which showed significant deviation from the full occupancy with the value 0.53(2). Therefore, in the final least-squares cycles all positions were assumed to be fully occupied with exception of this Cu position, for which the occupancy was fixed at 0.50. Thus, the compound has the composition $Cu_4Sn_7S_{16}$, corresponding to the Cu_2S mole proportion of 0.2222 in the pseudobinary $Cu_2S–SnS_2$ system. The refinement resulted in the conventional and weighted residuals $R = 0.018$ and $wR(F^2) = 0.040$ for 36 variables and 522 structure factors. Final difference Fourier map showed the highest and lowest electron densities of 0.88 and -1.86 e Å^{-3}, respectively, which were too close to the

TABLE 1
Some Data and Results of the Structure Determinations of
$Cu_4Sn_7S_{16}$ and Cu_2SnS_3

	$Cu_4Sn_7S_{16}$	Cu_2SnS_3
Chemical formula	$Cu_4Sn_7S_{16}$	Cu_2SnS_3
Formula weight	1597.95	341.95
Crystal dimension (mm)	$0.12 \times 0.08 \times 0.02$	$0.07 \times 0.10 \times 0.08$
Space group	R-$3m$ (No. 166)	I-$42m$ (No. 121)
Lattice constants		
a (Å)	7.372(1)	5.413(1)
c (Å)	36.010(7)	10.824(1)
Volume (Å^3)	1694.8(5)	317.15(9)
Z	3	16/6
Calculated density (g cm^{-3})	4.697	4.774
Temperature of data collection (K)	293	293
Wavelength (λMoKα) (Å)	0.71073	0.71073
Linear absorption coefficient μ (cm^{-1})	127.45	151.90
Transmission factors	0.463–0.822	0.419–0.496
Scan type	ω–2θ	ω–2θ
Scan speed	Variable	Variable
Scan range	$(0.8 + 0.35 \tan\theta)$	$(0.6 + 0.35 \tan\theta)$
2θ (max)	60°	70°
Range in hkl	-10–0, -8–10, ± 50	0–8, 0–8, ± 17
Total number of reflections	3515	1672
Unique reflections	672	399
Inner residual	$R_i = 0.049$	$R_i = 0.051$
Reflections with $F_o^2 > 2\sigma(F_o^2)$	522	281
Number of variables	36	16
Secondary extinction coefficient	0.00039(2)	0.030(2)
S (Goodness-of-fit on F^2)	1.110	0.974
Weighting scheme	$w = 1/[\sigma^2(F^2) + (0.013P)^2 + 8.485P]$ here P = $(F_o^2 + 2F_c^2)/3$	$w = 1/[\sigma^2(F^2) + (0.030P)^2]$
$R[F^2 > 2\sigma(F^2)]$	0.018	0.030
$wR(F^2)$	0.040	0.069
$(\Delta/\sigma)_{max}$	0.001	0.000

Cu2 position (0.55 and 0.81 Å, respectively) to be suitable for the accommodation of any additional atoms. It should be pointed out that this refinement results in a six-coordinated Cu3 site, which is uncommon. Refinement of this Cu position as a Sn atom leads to a formula of $Cu_9Sn_{22.83}S_{48}$ with the Sn occupancy of about 61%. It is clear that charge neutrality could not be obtained for such

a formula. In separate least-squares cycles, Cu and Sn were put together in this site with the constraint that their positional and thermal parameters are equal and the total occupation for this site is 1.0. The refinement of population parameters leads to a Cu/Sn ratio of 0.997(13)/0.003(13). Therefore, in the final refinement, only the Cu atom is assigned to this site, which gives a reasonable formula.

For Cu_2SnS_3, the space group I-$42m$ does not permit the assignment of copper and tin atoms to different sites within the limitation of eight metal atoms/unit cell. As no evidence of a supercell was found, it must be presumed that the copper and tin atoms are disordered over the metal sites. Refinement of the atomic occupancies indicates that one metal site (2a) is fully occupied by the copper atom, and the other two sites (2b and 4d) are clearly shared by tin and copper atoms. Therefore, in the final least-squares cycles the Sn and Cu atoms were allowed to disorder over these two positions with the constraints that the Sn and Cu occupancies at a given site sum to unity, that they have the same thermal parameters at a given site, and that the charge balance is fitted. The final R value is 0.030 for 281 reflections and 16 variables, and the final difference Fourier map is nearly flat with the highest and lowest electron densities 0.80 and -0.95 e Å^{-3}, respectively. The compound has the composition $Cu_{2.665(7)}Sn_{1.335(7)}S_4$ ($Z = 2$), corresponding to Cu_2SnS_3 ($Z = 16/6$). Refinement of Flack parameter gives a value of $-0.09(6)$, indicating that the absolute structure is correct. As a further test of this model, an alternative with complete disorder of the metal atoms over three kinds of positions (2a, 2b, and 4d) was tested, no final results were available because the refinement was unstable. Thus the model with Sn/Cu disorder confined to positions 2b and 4d is in good agreement with the diffraction data, and gives results that appear physically reasonable. The final positional, the equivalent isotropic and anisotropic displacement parameters of both compounds are given in Tables 2 and 3, respectively. Listings of the structure factors are available from the authors.

TABLE 2
Atomic Coordinates, Equivalent Isotropic and Anisotropic Displacement Parameters (Å^2) for $Cu_4Sn_7S_{16}$

Atom	Site type	x	y	z	U_{eq}	U_{11}	U_{22}	U_{33}	U_{23}	U_{13}	U_{12}
Sn1	18h	0.5017(1)	0.4983(1)	0.2513(1)	0.011(1)	0.011(1)	0.011(1)	0.013(1)	0.001(1)	$-0.001(1)$	0.006(1)
Sn2	3b	0	0	1/2	0.012(1)	0.013(1)	0.013(1)	0.008(1)	0	0	0.007(1)
Cu1	6c	0	0	0.1884(1)	0.016(1)	0.017(1)	0.017(1)	0.014(1)	0	0	0.009(1)
Cu2	6c	0	0	0.2945(1)	0.039(1)	0.013(1)	0.013(1)	0.090(1)	0	0	0.006(1)
Cu3	3a	0	0	0	0.054(1)	0.074(1)	0.074(1)	0.014(1)	0	0	0.037(1)
S1	18h	0.4937(1)	0.5063(1)	0.1244(1)	0.010(1)	0.010(1)	0.010(1)	0.009(1)	0.000(1)	0.000(1)	0.006(1)
S2	18h	0.5074(1)	0.4926(1)	0.3760(1)	0.011(1)	0.010(1)	0.010(1)	0.012(1)	0.001(1)	$-0.001(1)$	0.005(1)
S3	6c	0	0	0.1239(1)	0.010(1)	0.011(1)	0.011(1)	0.009(1)	0	0	0.006(1)
S4	6c	0	0	0.3756(1)	0.010(1)	0.010(1)	0.010(1)	0.010(1)	0	0	0.005(1)

Notes. The occupation factor of Cu1 is 0.50. U_{eq} is defined as one-third of the trace of the orthogonalized U_{ij} tensor. The anisotropic displacement factor exponent takes the form $-2\pi^2(h^2a^{*2}U_{11} + \cdots + 2hka^*b^*U_{12})$.

TABLE 3
Atomic Coordinates, Equivalent Isotropic and Anisotropic Displacement Parameters (Å^2) for Cu$_2$SnS$_3$

Atom	Site type	x	y	z	U_{eq}	U_{11}	U_{22}	U_{33}	U_{23}	U_{13}	U_{12}
M1	4d	0	1/2	1/4	0.019(1)	0.019(1)	0.019(1)	0.018(1)	0	0	0
M2	2b	0	0	1/2	0.019(1)	0.018(1)	0.018(1)	0.021(1)	0	0	0
Cu	2a	0	0	0	0.022(1)	0.020(1)	0.020(1)	0.024(1)	0	0	0
S	8i	0.2461(1)	0.2461(1)	0.1231(1)	0.015(1)	0.015(1)	0.015(1)	0.015(1)	− 0.001(1)	− 0.001(1)	− 0.001(1)

Notes. M1 = 43.6(2) at.% Sn + 56.4(2) at.% Cu, M2 = 46.3(3) at.% Sn + 53.7(3) at.% Cu. U_{eq} is defined as one-third of the trace of the orthogonalized U_{ij} tensor. The anisotropic displacement factor exponent takes the form $− 2\pi^2(h^2a^{*2}U_{11} + \cdots + 2hka^*b^*U_{12})$.

DISCUSSION

Cu$_4$Sn$_7$S$_{16}$ crystallizes in a new structure type of trigonal system (Pearson symbol hR81). Its crystal structure is characterized by a three-dimensional framework, which is closely related to that of spinel (MgAl$_2$O$_4$ type) (15). The strong X-ray powder diffraction peaks of this compound could be indexed as a spinel structure with a pseudocubic unit cell of about $a_c \approx 10.4$ Å. The approximate dimensional relations are: $a = b = 7.372$ Å $= \sqrt{2} \times a_c/2$, and $c = 36.010$ Å $= 2 \times \sqrt{3} \times a_c$. In fact, a is one-half of the [110] vector of the cubic cell and c corresponds to the double of its [111] vector. The space group R-$3m$ of Cu$_4$Sn$_7$S$_{16}$ is actually a *translationengleiche* subgroup of the group Fd-$3m$ adopted by spinel. A comparison of the atomic parameters of Cu$_4$Sn$_7$S$_{16}$ (Table 2) with those of MgAl$_2$O$_4$ (15) indicates that the tetrahedral sites of the spinel structure are split into two nonequivalent groups, 6c and 6c, with 3m symmetry, and they are occupied by Cu2 and statistically by Cu1, respectively. The octahedral sites are split into three nonequivalent sets, 18h, 3b, and 3a, with symmetry m, −3m, and −3m, and accommodated by Sn1, Sn2, and Cu3, respectively. Similarly, the sulfur atoms are divided into four different groups, 18h, 18h, 6c, and 6c, with symmetry m or 3m. The 12-layer sulfur atoms form a slightly distorted cubic close-packed arrangement along the c-axis in sequence ...ABC.... The Cu and Sn atoms are distributed in an ordered manner over the tetrahedral and octahedral voids between the S-layers and some of them are displaced from the centers of their coordination polyhedra, which results in a lowering of the space-group symmetry. Figure 1 shows a portion of the structure, according to the method of representation for spinel used by Baltzer *et al.* (16), and Fig. 2 gives a perspective view of the unit cell. As can be seen, the Sn- and Cu3-centered octahedra are interconnected by edge sharing and they are connected to Cu1- or Cu2-centered tetrahedra by corner sharing. The Cu1- and Cu2-centered tetrahedra are separated from each other.

Table 4 lists the selected bond distances and angles concerning the coordination geometries of the cation-centered sulfur polyhedra in Cu$_4$Sn$_7$S$_{16}$. The Sn–S bond lengths vary in a narrow range 2.5095(7)–2.5956(7) Å and the 90° octahedral angles for SnS$_6$ units are in the range 86.19(5)–92.79(3)°, indicating that the octahedral environments are slightly distorted. The average Sn–S bond distances are 2.564(1) Å for Sn1 and 2.552(1) Å for Sn2, respectively. They are in excellent agreement with those found in other Sn^{4+}-containing sulfides such as: 2.570(4) Å in La$_2$SnS$_5$ (17), 2.566(2) Å in Ag$_{3.8}$Sn$_3$S$_8$ (2), and 2.56(1) Å in CuSn$_{3.75}$S$_8$ (8).

The tetrahedron around Cu1 is almost regular, with the S–Cu–S angles being near the tetrahedral value and the Cu–S distances exhibiting a narrow range [2.322(2)–2.330(1) Å]. The average Cu–S distance of 2.328(2) Å compares well with those generally found in ternary or quaternary copper chalcogenides with similar coordination around Cu$^+$: 2.343(2) and 2.333(1) Å in Cu$_4$TiS$_4$ (18), 2.320(1) Å in Cu$_2$FeSn$_3$S$_8$ (19), and 2.307(1) Å in KCuZrS$_3$ (20).
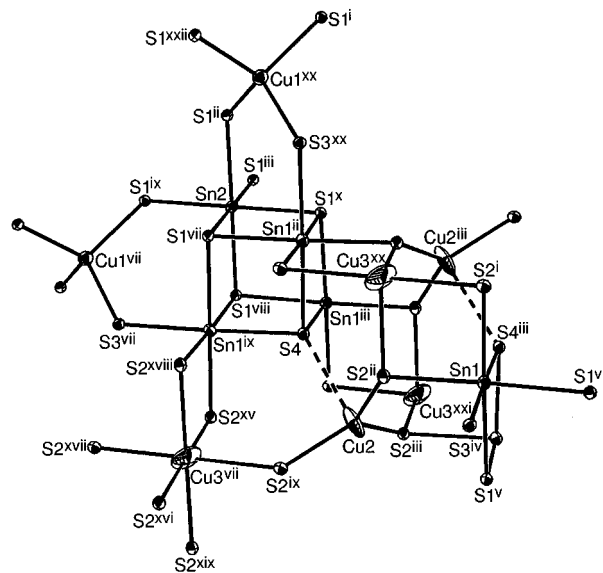

FIG. 1. Portion of the structure of Cu$_4$Sn$_7$S$_{16}$ with the atomic numbering scheme. The dashed lines represent weak Cu2...S4 interactions of 2.922(3) Å and the symmetry codes here are the same as those in Table 4. Displacement ellipsoids are shown at the 50% probability level.
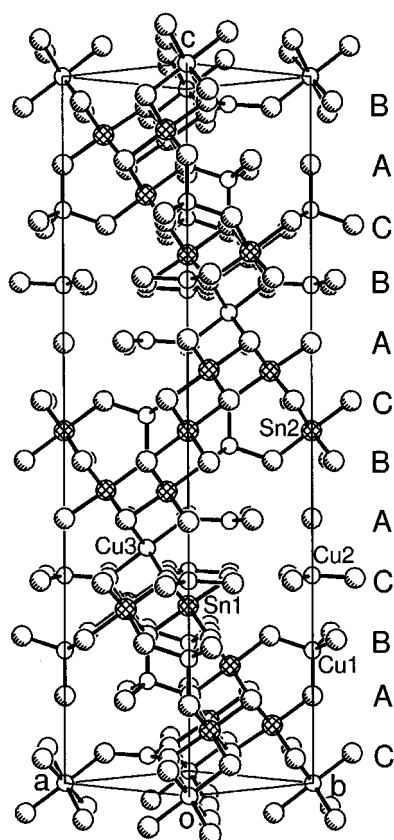
FIG. 2. View of the $Cu_4Sn_7S_{16}$ structure along [110] with the unit cell outlined. The open circles are Cu atoms, the cross-hatched circles are Sn atoms, and the partly shaded circles are S stoms.

TABLE 4
Selected Bond Lengths (Å) and Angles (°) for $Cu_4Sn_7S_{16}$

Sn1–S2^{i}	2.5095(7)	Cu1–S3	2.322(2)
Sn1–S2^{ii}	2.5095(7)	Cu1–S1^{iv}	2.330(1)
Sn1–S4^{iii}	2.582(1)	Cu1–S1^{v}	2.330(1)
Sn1–S3^{iv}	2.590(1)	Cu1–S1^{xi}	2.330(1)
Sn1–S1^{v}	2.5956(7)	Cu2–S2^{iii}	2.227(1)
Sn1–S1^{vi}	2.5956(7)	Cu2–S2^{ix}	2.227(1)
Sn2–S1^{iii}	2.552(1)	Cu2–S2^{ii}	2.227(1)
Sn2–S1^{vii}	2.552(1)	Cu3–S2^{iv}	2.549(1)
Sn2–S1^{ii}	2.552(1)	Cu3–S2^{xii}	2.549(1)
Sn2–S1^{viii}	2.552(1)	Cu3–S2^{xi}	2.549(1)
Sn2–S1^{ix}	2.552(1)	Cu3–S2^{xiii}	2.549(1)
Sn2–S1^{x}	2.552(1)	Cu3–S2^{v}	2.549(1)
		Cu3–S2^{xiv}	2.549(1)

S2^{i}–Sn1–S2^{ii}	89.14(5)	S1^{ii}–Sn2–S1^{x}	91.95(3)
S2^{i}–Sn1–S4^{iii}	92.79(3)	S1^{viii}–Sn2–S1^{x}	88.05(3)
S2^{ii}–Sn1–S4^{iii}	92.79(3)	S1^{ix}–Sn2–S1^{x}	180.0
S2^{i}–Sn1–S3^{iv}	88.58(3)	S3–Cu1–S1^{iv}	108.57(5)
S2^{ii}–Sn1–S3^{iv}	88.58(3)	S3–Cu1–S1^{v}	108.57(5)
S4^{iii}–Sn1–S3^{iv}	178.09(5)	S1^{iv}–Cu1–S1^{v}	110.36(5)
S2^{i}–Sn1–S1^{v}	178.31(3)	S3–Cu1–S1^{xi}	108.57(5)
S2^{ii}–Sn1–S1^{v}	92.33(3)	S1^{iv}–Cu1–S1^{xi}	110.36(5)
S4^{iii}–Sn1–S1^{v}	87.97(3)	S1^{v}–Cu1–S1^{xi}	110.36(5)
S3^{iv}–Sn1–S1^{v}	90.64(3)	S2^{iii}–Cu2–S2^{ix}	119.62(1)
S2^{i}–Sn1–S1^{vi}	92.33(3)	S2^{iii}–Cu2–S2^{ii}	119.62(1)
S2^{ii}–Sn1–S1^{vi}	178.31(3)	S2^{ix}–Cu2–S2^{ii}	119.62(1)
S4^{iii}–Sn1–S1^{vi}	87.97(3)	S2^{iv}–Cu3–S2^{xii}	180.0
S3^{iv}–Sn1–S1^{vi}	90.64(3)	S2^{iv}–Cu3–S2^{xi}	87.40(3)
S1^{v}–Sn1–S1^{vi}	86.19(5)	S2^{xii}–Cu3–S2^{xi}	92.60(3)
S1^{iii}–Sn2–S1^{vii}	180.0	S2^{iv}–Cu3–S2^{xiii}	92.60(3)
S1^{iii}–Sn2–S1^{ii}	88.05(3)	S2^{xii}–Cu3–S2^{xiii}	87.40(3)
S1^{vii}–Sn2–S1^{ii}	91.95(3)	S2^{xi}–Cu3–S2^{xiii}	180.0
S1^{iii}–Sn2–S1^{viii}	91.95(3)	S2^{iv}–Cu3–S2^{v}	87.40(3)
S1^{vii}–Sn2–S1^{viii}	88.05(3)	S2^{xii}–Cu3–S2^{v}	92.60(3)
S1^{ii}–Sn2–S1^{viii}	180.0	S2^{xi}–Cu3–S2^{v}	87.40(3)
S1^{iii}–Sn2–S1^{ix}	88.05(3)	S2^{xiii}–Cu3–S2^{v}	92.60(3)
S1^{vii}–Sn2–S1^{ix}	91.95(3)	S2^{iv}–Cu3–S2^{xiv}	92.60(3)
S1^{ii}–Sn2–S1^{ix}	88.05(3)	S2^{xii}–Cu3–S2^{xiv}	87.40(3)
S1^{viii}–Sn2–S1^{ix}	91.95(3)	S2^{xi}–Cu3–S2^{xiv}	92.60(3)
S1^{iii}–Sn2–S1^{x}	91.95(3)	S2^{xiii}–Cu3–S2^{xiv}	87.40(3)
S1^{vii}–Sn2–S1^{x}	88.05(3)	S2^{v}–Cu3–S2^{xiv}	180.0

Note. Symmetry codes: (i) $y + 1/3$, $-x + y + 2/3$, $-z + 2/3$; (ii) $x - y + 1/3$, $x - 1/3$, $-z + 2/3$; (iii) $-x + 1/3$, $-y + 2/3$, $-z + 2/3$; (iv) $-x + 2/3$, $-y + 1/3$, $-z + 1/3$; (v) $y - 1/3$, $-x + y + 1/3$, $-z + 1/3$; (vi) $x - y + 2/3$, $x + 1/3$, $-z + 1/3$; (vii) $x - 1/3$, $y - 2/3$, $z + 1/3$; (viii) $-x + y - 1/3$, $-x + 1/3$, $z + 1/3$; (ix) $y - 2/3$, $-x + y - 1/3$, $-z + 2/3$; (x) $-y + 2/3$, $x - y + 1/3$, $z + 1/3$; (xi) $x - y - 1/3$, $x - 2/3$, $-z + 1/3$; (xii) $x - 2/3$, $y - 1/3$, $z - 1/3$; (xiii) $-x + y + 1/3$, $-x + 2/3$, $z - 1/3$; (xiv) $-y + 1/3$, $x - y - 1/3$, $z - 1/3$; (xv) $x - 1$, $y - 1$, z; (xvi) $-x + 1/3$, $-y - 1/3$, $-z + 2/3$; (xvii) $-y$, $x - y - 1$, z; (xviii) $-x + y$, $-x$, z; (xix) $x - y - 2/3$, $x - 4/3$, $-z + 2/3$; (xx) $x + 2/3$, $y + 1/3$, $z + 1/3$; (xxi) $x - 1/3$, $y + 1/3$, $z + 1/3$; (xxii) $-x + 4/3$, $-y + 2/3$, $-z + 2/3$.

Two different coordination geometries may be used to characterize the environment of an Cu2 atom: (i) The Cu2 site may be described as a triangular site in which the copper atom is displaced slightly out of the plane through three S2 atoms by 0.139(2) Å. The Cu2–S2 distances are 2.227(1) Å and S2–Cu2–S2 bond angles 119.62(1)°. These values are closely comparable to those for CuS_3 coordination found in $Cu_2U_3S_7$ (21) (2.219(2) Å and 119.84°). However, the Cu2–S distances are slightly shorter than those usually found for such a coordination: 2.33(1) Å in $TlCu_3S_2$ (22), 2.321(9) Å in Cu_4SnS_4 (7). (ii) The Cu2 site may also be described as a distorted tetrahedron site made up of three S2 and one S4 atoms, but in this case one Cu–S bond length [Cu2–S4 of 2.922(3) Å] is very long compared to the others. The existence of such an elongated Cu–S bond may be responsible for the shortening of the Cu–S distances on the opposite side.

Cu3 has an unusual octahedral environment with Cu–S distances of 2.549(1) Å. Indeed, with a $3d^{10}4s^0$ electronic configuration, Cu^+ favors a linear or tetrahedral surrounding, the latter being common in sulfides. In order to examine the oxidation state of copper ions in $Cu_4Sn_7S_{16}$, XPS measurements were done on the powder samples of this compound. Figure 3 illustrates the Cu 2p core level spectrum. The observed values of the binding energies for Cu $2p_{3/2}$ and Cu $2p_{1/2}$ are in good agreement with those in the
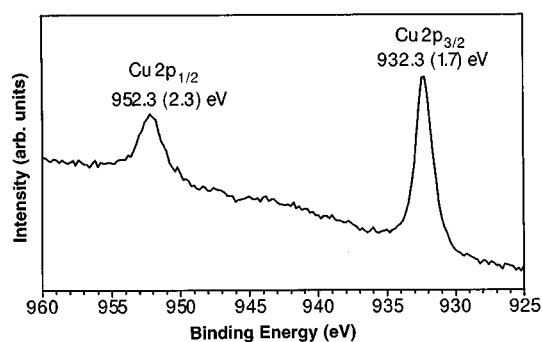
FIG. 3. Cu 2p core level XPS spectrum of $Cu_4Sn_7S_{16}$. The binding energy positions (with the corresponding FWHM in parentheses) are indicated in the figure.

literature (23). The full width at half maximum (FWHM) calculated for Cu $2p_{3/2}$ and Cu $2p_{1/2}$ are 1.7 and 2.3 eV, respectively, which are also in good agreement with the reported values for Cu^+ (23). Besides, the Cu $2p_{3/2}$ satellite peaks, which are usually centered at about 942 eV and characteristic of Cu^{2+} (24), are missing in Fig. 3. Therefore, we may conclude that only Cu^+ is present in this compound. XPS analysis also revealed the normal valence states for Sn and S atoms. The Sn $3d_{5/2}$ and Sn $3d_{3/2}$ binding energies, 486.8 and 495.2 eV, respectively, compared well with those observed in SnS_2 (25), and S core level spectrum shows the binding energies of 161.8 and 162.9 eV for $2p_{3/2}$ and $2p_{1/2}$ states, respectively, very similar to those observed in chalcopyrite $CuFeS_2$ (26).

In this structure, two Sn and four S positions are well defined, as revealed by their full local site occupancies and the smaller equivalent thermal factors (Table 2). Of three Cu atoms, the Cu1 site has almost a spherical displacement ellipsoid, but it is half-occupied. This is a common occurrence in such a system. For example, the half-occupied tetrahedral Cu atom in $CsCuCe_2S_6$ (27) has the comparable equivalent thermal parameter [B_{eq} of 1.7(2) $Å^2$] and Cu–S bond lengths [average value of 2.353(4) Å]. The displacement ellipsoid of the Cu2 atom is far from spherical, the values of U_{33} being much bigger than those of U_{11} and U_{22}. This may be explained by its coordination geometry. As mentioned above, the Cu2 site may be regarded as a tetrahedral site in which the Cu2 atom bonds with three S2 atoms [average distances 2.227(1) Å] along the xy plane and one S4 atom [2.922(3) Å] along the z direction. Thus Cu2 atom is strongly anisotropic along the z direction. The Cu3 site has an octahedral S environment, which is unexpected. The larger thermal factors of this atom may be associated with its greater mobility in the xy plane, which can be seen from the relatively large U_{11} and U_{22} values in Table 2. A similar situation was previously observed in the compounds $CuCrP_2S_6$ (28), $CuVP_2S_6$ (29), and $AgScP_2S_6$ (30), where the high B_{eq} values of closed shell Cu^+ and Ag^+ were

explained not as corresponding to strong vibrations, but to a shift of Cu^+ or Ag^+ from the octahedral center to off-center positions. For instance, in $CuVP_2S_6$, three different identifiable sites were found, one near the center of the Cu^+ octahedron, another close to the triangular face of this octahedron, and the last one in a van der Waals tetrahedral position. In the $AgScP_2S_6$ structure, only one octahedral Ag^+ site was found, and its abnormally large thermal parameter indicates a tendency to move away from the center of the octahedra, which was attributed to a second-order Jahn-Teller coupling between the filled silver e_g manifold and the empty s orbital. The Cu3 atom in $Cu_4Sn_7S_{16}$ is very similar to the Ag atom in $AgScP_2S_6$ and a similar explanation may also be reasonable for our case.

In the pseudobinary Cu_2S–SnS_2 system, $CuSn_{3.75}S_8$ has a defect cubic spinel-type structure with space group F-$43m$ (8). Its formula can be written as $(Cu_{0.5}\square_{0.5})(Sn_{1.875}\square'_{0.125})S_4$. Thus, half of the tetrahedral sites and 15/16 of the octahedral sites are occupied by Cu^+ and Sn^{4+} ions, respectively. Although $Cu_4Sn_7S_{16}$ has a rhombohedral symmetry, its formula can also be similarly represented as $(Cu_{0.75}\square_{0.25})(Sn_{1.75}Cu_{0.25})S_4$. In the unit cell, both 3/4 of the tetrahedral sites and 1/8 of the octahedral sites are occupied by Cu^+, while 7/8 of the octahedral sites are occupied by Sn^{4+} ions. Therefore, its crystal structure may be described as a defect variant of the spinel-type.

Cu_2SnS_3 has the unit cell formula $Cu_{2.665(7)}Sn_{1.335(7)}S_4$ ($Z = 2$) and crystallizes with the tetragonal stannite [$Cu_2(Fe, Zn)SnS_4$] structure (31). The composite atoms M1 [43.6(2) at.% Sn + 56.4(2) at.% Cu] and M2 [46.3(3) at.% Sn + 53.7(3) at.% Cu] occupy the positions of the Cu and Sn atoms of stannite, respectively, and the rest of Cu atoms in Cu_2SnS_3 occupy those of the corresponding (Fe, Zn) atoms. As Cu and Sn have different sizes, disorder between them is unique. However, the crystal of Cu_2SnS_3 was obtained by quenching from 700°C. At this temperature, such a copper distribution may be possible. Moh (5) previously observed under the microscope a complete solid solution range between this phase and stannite (Cu_2FeSnS_4) and concluded that this phase crystallizes in a tetragonal lattice similar to that of stannite. Our structural refinement confirms his conclusion. The crystal of Cu_2SnS_3 showed narrow and symmetric diffraction peaks during reflection scans and the tetragonal lattice parameters obtained by the diffractometer [$a = 5.4126(1)$, $c = 10.8239(4)$ Å] are reliable with very small standard deviations. The fact that the diffraction peaks were not split and the systematic absences were consistent with I-$42m$ symmetry excludes the possibility of twinning. Attempts to refine the structure in lower-symmetry space groups with an ordered distribution of Cu and Sn atoms were unsuccessful.

In the structure, all metal atoms are fixed on special positions and each is surrounded by four sulfur atoms forming a distorted tetrahedron. Each sulfur atom is

TABLE 5
Selected Bond Lengths (Å) and Angles (°) for Cu$_2$SnS$_3$

|			
M1–S^i	2.3562(6)	M2–S^{vi}	2.356(1)
M1–S^{ii}	2.3562(6)	M2–S^{ii}	2.356(1)
M1–S^{iii}	2.3562(6)	Cu–S	2.307(1)
M1–S	2.3562(6)	Cu–S^{vii}	2.307(1)
M2–S^{iv}	2.356(1)	Cu–S^{ix}	2.307(1)
M2–S^v	2.356(1)	Cu–S^{viii}	2.307(1)
S^i–M1–S^{ii}	108.65(4)	S^{iv}–M2–S^{ii}	108.64(2)
S^i–M1–S^{iii}	109.88(2)	S^v–M2–S^{ii}	111.15(5)
S^{ii}–M1–S^{iii}	109.88(2)	S^{vi}–M2–S^{ii}	108.64(2)
S^i–M1–S	109.88(2)	S–Cu–S^{vii}	109.46(2)
S^{ii}–M1–S	109.88(2)	S–Cu–S^{ix}	109.49(5)
S^{iii}–M1–S	108.65(4)	S^{vii}–Cu–S^{ix}	109.46(2)
S^{iv}–M2–S^v	108.64(2)	S–Cu–S^{viii}	109.46(2)
S^{iv}–M2–S^{vi}	111.15(5)	S^{vii}–Cu–S^{viii}	109.49(5)
S^v–M2–S^{vi}	108.64(2)	S^{ix}–Cu–S^{viii}	109.46(2)

Note. Symmetry codes: (i) $-y + 1/2$, $x + 1/2$, $-z + 1/2$; (ii) $y - 1/2$, $-x + 1/2$, $-z + 1/2$; (iii) $-x$, $-y + 1$, z; (iv) $-x + 1/2$, $-y + 1/2$, $z + 1/2$; (v) $-y + 1/2$, $x - 1/2$, $-z + 1/2$; (vi) $x - 1/2$, $y - 1/2$, $z + 1/2$; (vii) $-y$, x, $-z$; (viii) y, $-x$, $-z$; (ix) $-x$, $-y$, z.

tetrahedrally bonded to two M1, one M2, and one Cu atoms. Selected bond lengths and angles are collected in Table 5. The Cu–S distance 2.307(1) Å is in good agreement with that observed in the chalcopyrite structure [2.302(1) Å] (32). The M1–S distance 2.3562(6) Å is equal to that of M2–S [2.356(1) Å] within experimental error, and both are intermediate between 2.320(2) Å of Cu–S and 2.411(2) Å of Sn–S bond lengths observed in stannite (31). Figure 4 shows the

unit cell structure and atomic coordination arrangements. A comparison of this figure with the corresponding ones in stannite indicates that the configurations of the coordination tetrahedra are slightly different in both structures. For Cu$_2$SnS$_3$, the smaller copper atom at the origin of the unit cell gives rise to a displacement of the coordinating sulfur toward this position, thereby forming almost an ideal CuS$_4$ tetrahedron [angles 109.46(2)°–109.49(5)° in comparison with 107.0(1)°–110.7(1)° for Fe/Zn site in stannite]. Similarly, the coordination tetrahedron around M1 is less distorted than it is in stannite [angles 108.65(4)°–109.88(2)° as opposed to 108.1(1)°–112.3(1)° for Cu site in stannite] and the coordination tetrahedron around M2 is more distorted with a wide angle range of 108.64(2)°–111.15(5)°. The thermal parameters of Cu [$B_{eq} = 8\pi^2 U_{eq} = 1.74(8)$ Å^2] and S [$B_{eq} = 1.18(8)$ Å^2] atoms are quite comparable to those observed in the isotypic compound Cu$_2$CdSnS$_4$ (1.64 and 1.16 Å^2, respectively) (33), but they are higher than those in stannite. This probably reflects the overall differences in their diffraction data. Although we could not compare the thermal parameters of the mixed sites M1 and M2 with those in the literature, the relative magnitudes $U_{eq}(Cu) > U_{eq}(Sn, Cu)$ in Cu$_2$SnS$_3$ follow the general pattern $B_{eq}(Cu) > B_{eq}(Sn)$ observed in stannite and the other chalcopyrite-like structures.

There are no S–S bondings in Cu$_4$Sn$_7$S$_{16}$ and Cu$_2$SnS$_3$; the shortest S...S nonbonded contacts are 3.522(2) and 3.768(2) Å, respectively, significantly longer than the 2.07 Å, expected for S–S single bonds (34). Therefore, both compounds may be formulated as Cu$_4^{1+}$Sn$_7^{4+}$S$_{16}^{2-}$ and
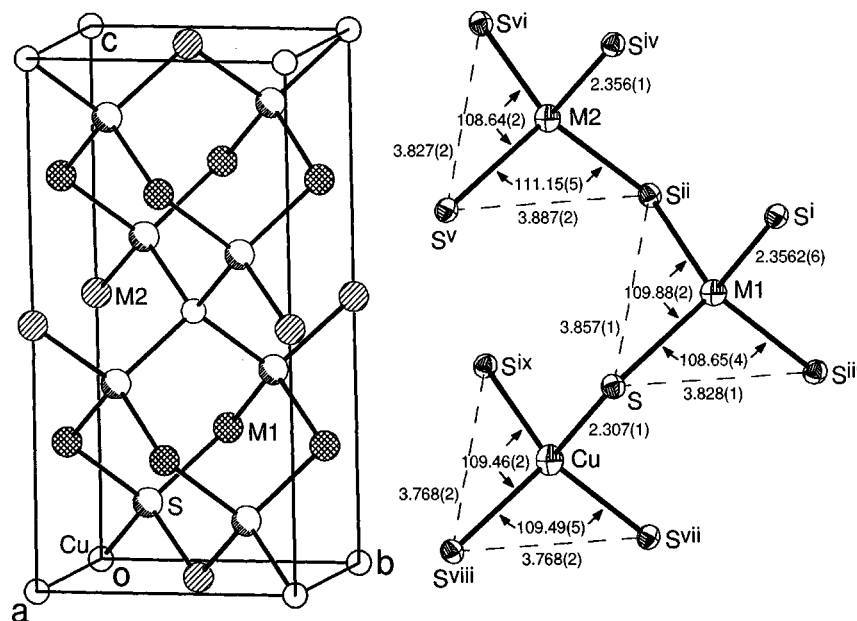
FIG. 4. Unit cell structure and atomic coordinations of Cu$_2$SnS$_3$. The interatomic distances are in angstroms and angles in degrees. The symmetry codes here are the same as those in Table 5 and displacement ellipsoids are shown at the 50% probability level.
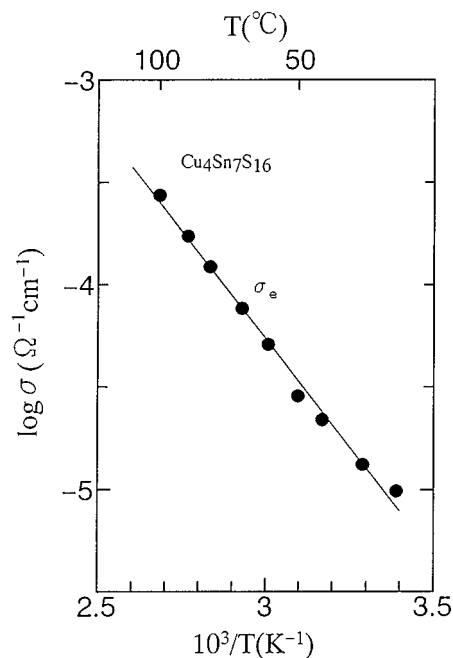
FIG. 5. Electrical conductivity of $Cu_4Sn_7S_{16}$ versus temperature.

$Cu_2^{1+}Sn^{4+}S_3^{2-}$, the closed-shell system that one would expect to exhibit insulating or semiconducting properties. The electric conductivity measurements of $Cu_4Sn_7S_{16}$ were performed in the cell arrangement Pt/sample/Pt. Experimental results were plotted in Fig. 5 as a function of temperature. Data indicate clearly a typical semiconductor behavior. The electric conductivity of $Cu_4Sn_7S_{16}$ is $\log \sigma \approx -5.01$ at 22°C and increases linearly to -3.56 at 100°C with an activation energy of 0.42 eV. The supplemental DSC measurement revealed no phase transition in this temperature range. The electrical properties of Cu_2SnS_3 have been investigated previously by Khanafer et al. (35), and it also exhibits the expected semiconducting behavior.

ACKNOWLEDGMENTS

REFERENCES

1. W. F. Kuhs, R. Nitsche, and K. Scheunemann, *Mater. Res. Bull.* **14,** 241 (1979).
2. O. Amiel, D. C. Frankel, and H. Wada, *J. Solid State Chem.* **116,** 409 (1995).
3. M. Khanafer, J. Rivet, and J. Flahaut, *Bull. Soc. Chim. Fr.* 2670 (1974).
4. N. Wang, *Neues Jahrb. Mineral. Monatsh.* 424 (1974).
5. G. H. Moh, *in* "Sulphide Systems Containing Sn," Year book 62, p. 197. Carnegie Inst., Washington, 1963.
6. G. H. Moh, *Chem. Erde* **34,** 1 (1975).
7. S. Jaulmes, J. Rivet, and P. Laruelle, *Acta Crystallogr. Sect. B* **33,** 540 (1977).
8. S. Jaulmes, M. Julien-Pouzol, J. Rivet, J. C. Jumas, and M. Maurin, *Acta Crystallogr. Sect. B* **38,** 51 (1982).
9. H. Hahn, W. Klingen, P. Ness, and H. Schulze, *Naturwissenschaftea* **53,** 18 (1966).
10. P. Villars and L. D. Calvert, "Pearson's Handbook of Crystallographic Data for Intermetallic Phases." Materials Information Society, Materials Park, OH, 1991.
11. N. Wang, *Neues Jahrb. Mineral. Monatsh.* 166 (1975).
12. B. A. Frenz and Associates, "SDP for Windows Reference Manual." College Station, TX, 1995.
13. A. Altomare, G. Cascarano, C. Giacovazzo, and A. Guagliardi, *J. Appl. Crystallogr.* **26,** 343 (1993).
14. G. M. Sheldrick, "SHELXL93, a Program for the Refinement of Crystal Structures." University of Göttingen, Germany, 1993.
15. N. G. Zorina and S. S. Kvitka, *Soviet Phys. Crystallogr.* **13,** 599 (1969).
16. P. K. Baltzer, P. J. Wojtowicz, M. Robbins, and E. Lopatin, *Phys. Rev.* **151,** 367 (1966).
17. S. Jaulmes, *Acta Crystallogr. Sect. B* **30,** 2283 (1974).
18. K. O. Klepp and D. Gurtner, *J. Alloys Compd.* **243,** 19 (1996).
19. J. C. Jumas, E. Philippot, and M. Maurin, *Acta Crystallogr. Sect. B* **35,** 2195 (1979).
20. M. F. Mansuetto, P. M. Keane, and J. A. Ibers, *J. Solid State Chem.* **101,** 257 (1992).
21. A. Daoudi, M. Lamire, J. C. Levet, and H. Noël, *J. Solid State Chem.* **123,** 331 (1996).
22. K. Klepp and K. Yvon, *Acta Crystallogr. Sect. B* **36,** 2389 (1980).
23. J. Llanos, A. Buljan, C. Mujica, and R. Ramírez, *J. Alloys Compd.* **234,** 40 (1996).
24. L. D. Partain, R. A. Schneider, L. F. Donaghey, and P. S. McLeod, *J. Appl. Phys.* **57,** 5056 (1985).
25. A. R. H. F. Ettema and C. Haas, *J. Phys. Condens. Matter* **5,** 3817 (1993).
26. I. Nakai, Y. Sugitani, K. Nagashima, and Y. Niwa, *J. Inorg. Nucl. Chem.* **40,** 789 (1978).
27. A. C. Sutorik, J. Albritton-Thomas, T. Hogan, C. R. Kannewurf, and M. G. Kanatzidis, *Chem. Mater.* **8,** 751 (1996).
28. P. Colombet, A. Leblanc, M. Danot, and J. Rouxel, *J. Solid State Chem.* **41,** 174 (1982).
29. E. Durand, G. Ouvrard, M. Evain, and R. Brec, *Inorg. Chem.* **29,** 4916 (1990).
30. S. Lee, P. Colombet, G. Ouvrard, and R. Brec, *Inorg. Chem.* **27,** 1291 (1988).
31. S. R. Hall, J. T. Szymanski, and J. M. Stewart, *Can. Mineral.* **16,** 131 (1978).
32. S. R. Hall and J. M. Stewart, *Acta Crystallogr. Sect. B* **29,** 579 (1973).
33. J. T. Szymanski, *Can. Mineral.* **16,** 147 (1978).
34. S. A. Sunshine, D. Kang, and J. A. Ibers, *J. Am. Chem. Soc.* **109,** 6202 (1987).
35. M. Khanafer, O. Gorochov, and J. Rivet, *Mater. Res. Bull.* **9,** 1543 (1974).
36. G. M. Sheldrick, "SHELXTL PC Version 4.1, an Integrated System for Solving, Refining, and Displaying Crystal Structures from Diffraction Data." Siemens Analytical X-Ray Instrument Inc., Madison, Wisconsin, 1990.